

Time-resolved picosecond absorption spectroscopy of the layered compound gallium selenide

S. S. Yao, J. Buchert, and R. R. Alfano

Ultrafast Spectroscopy and Laser Laboratory, Physics Department, The City College of New York, New York, New York 10031

(Received 26 February 1982)

The picosecond excite-and-probe absorption technique was used to study the relaxation process of photogenerated hot carriers in ϵ -GaSe at room temperature. The time dependence of the carrier temperature to relax to the lattice temperature was calculated from the absorption kinetic data. The carriers cooled at the rate of 30 K/ps. The dominant relaxation mechanism of the photogenerated hot carriers in GaSe is attributed to the emission of nonpolar optical phonons $A_1^{(1)}$. A smaller value for the deformation potential extracted from the measurements is attributed to the screening of hole-phonon interaction by the photogenerated carrier density.

I. INTRODUCTION

Time-resolved absorption and luminescence spectroscopy of semiconductors under intense excitation are subjects of current interest and are being investigated extensively. A layered compound which has interesting optical and electrical properties is gallium selenide (GaSe). It is transparent over a wide spectral range from 0.65 to 17.5 μm , and its large second-order susceptibility and birefringence makes it suitable for nonlinear optical processes. Excitons, electrons, and coupled excitation effects have been observed in the absorption and luminescence of GaSe at high intensity.¹ In layered semiconductors, the short-range interaction with optical phonons is the dominant carrier scattering mechanism² because of the large site dissymmetries and the large gradients of the atomic potentials. According to Schlueter³ the charge distribution of valence electrons (holes) will strongly couple to phonons involving vibrations which change the Ga-Ga bond length. The interaction of holes with nonpolar, fully symmetric, optical phonons $A_1^{(1)}$ governs both the Hall mobility of the carriers and the temperature shift of the direct energy gap of GaSe.⁴ Because the electron density corresponding to the conduction band is more diffuse⁴ than that corresponding to the valence band, the deformation potentials of the conduction band are expected to be significantly smaller than that of the valence band. The Hall mobilities of holes both along and perpendicular to the layers of GaSe are limited by homopolar optical-phonon scattering.⁵ This carrier-phonon coupling was also confirmed by the experimental data on the long-wavelength absorption tail which follows the Urbach rule.⁶ In fact, the $A_1^{(1)}$ phonon (135 cm^{-1}) is the strongest Raman mode, suggesting a strong carrier-phonon interaction.

In this Communication, the time-resolved absorption spectroscopy of ϵ -GaSe using the picosecond ex-

cite and probe technique has been measured. The absorption changes⁷ due to the relaxation of hot photogenerated carriers were fitted to obtain carrier temperature kinetics. We found that the emission of the nonpolar optical phonons $A_1^{(1)}$ (=16.7 meV) is the dominant mechanism to describe the absorption changes caused by the hot-carrier relaxation.

II. EXPERIMENTAL METHODS

A schematic diagram of the picosecond absorption apparatus can be found in Ref. 8. An 8-ps single pulse at 1060 nm is selected and amplified by 30 times to 30 mJ. Approximately 5% of the pulse is converted to the second harmonic at 530 nm while the 1060-nm pulse is reflected by a dielectric mirror and focused into a 15-cm-long CCl_4 cell to produce the supercontinuum (400 to 800 nm). The absorption kinetics subsequent to excitation can be followed by moving the delay prism across the time domain of interest, usually 500 ps with a time resolution of less than 10 ps. At the sample site, the probe pulse is divided into two pulses. One of these two probe pulses passes through the sample, and the other one passes above the sample. The two probe pulses are measured by a spectrograph coupled with a Hamamatsu television system and temporal analyzer. The spectral region investigated was between 580 to 640 nm. The pump pulse was polarized with $\vec{E} \perp c$ where the c axis of GaSe is normal to the layer. The sample thickness is about 20 μm . The excitation area on the sample is $1 \times 2 \text{ mm}^2$, and the incident pump energy is 800 μJ . The absorption constant of 530-nm light at room temperature is about $2 \times 10^3 \text{ cm}^{-1}$. Not all the photons were absorbed because of scattering. This is illustrated in Fig. 1 where the background absorption due to scattering below the band gap is 1.5 OD (optical density) instead of being zero. This

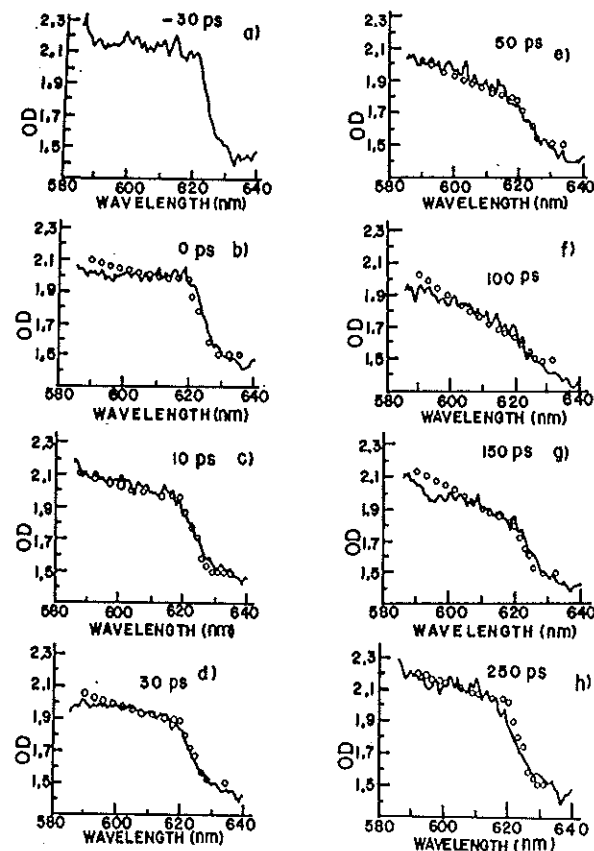


FIG. 1. Absorption curves at different time delays: Solid curves are experimental results and dots are theoretical fits to Eq. (1).

means that 97% of the pump photons are scattered and only 3% of the photons can be useful for the absorption above the band gap. The estimated optically generated electron-hole pairs are $\sim 7 \times 10^{18} \text{ cm}^{-3}$.

III. EXPERIMENTAL RESULTS

The absorption curves measured at different time delays from -30 to 250 ps are displayed in Fig. 1. The solid curves are the experimental results and the dots are the theoretical fits which will be discussed in the next section. Each absorption curve at certain time delay is the average of three absorption curves at about the same excitation intensity. The error for the solid curve is ± 0.1 OD. The salient features of the curves displayed in Fig. 1 are as follows: the absorption below 620 nm decreases in the first 100 ps, then increases to its original absorption value after 100 ps because of thermalization and recombination. The photoluminescence from GaSe excited by picosecond laser pulse consists of two emission bands⁹: one band is from spontaneous emission with a decay time of 300 ps and another band is from stimulated emission with a decay time of 100 ps when the carrier

density is $3 \times 10^{18} \text{ cm}^{-3}$. At $7 \times 10^{17} \text{ cm}^{-3}$, the spontaneous and stimulated bands are centered at 632 and 648 nm, respectively. The time-integrated stimulated emission intensity is very much larger than the spontaneous emission intensity. Therefore, the majority of photogenerated carriers are depleted because of the stimulated emission.

IV. DISCUSSION

The direct band gap of ϵ -GaSe at room temperature is 2.02 eV (613 nm) and the direct exciton energy is 2.00 eV (620 nm). In Fig. 1, the absorption at wavelength less than 620 nm is because of the direct band-gap absorption because the indirect absorption is weak.¹⁰ According to the calculations of Ugumori *et al.*,¹¹ the Mott transition in GaSe from the exciton state to the plasma state occurs at the carrier density $\eta = 4.8 \times 10^{17} \text{ cm}^{-3}$. This is also confirmed by our picosecond luminescence analysis⁹ for GaSe where we found $\eta_{\text{Mott}} \approx 3 \times 10^{17} \text{ cm}^{-3}$. In this Communication, the optically generated number of electron-hole pairs is $\sim 10^{19} \text{ cm}^{-3}$. Thus, we are operating in the electron-hole plasma regime. The band gap is renormalized and reduced to about 1.950 eV.⁹ Many-body effects due to electron-hole attraction at high-density account for the absorption change near the band edge of direct-gap semiconductors.^{7,12}

In this section, we will calculate the transient absorption changes resulting from hot carriers in thermal equilibrium. The absorption change at different time delays is fitted using the equation⁷:

$$\alpha = \alpha_0(1 - f_e)(1 - f_h) \quad (1)$$

The calculated curves are displayed in Fig. 1 by the circle dots, where α_0 is the absorption of the sample without excitation, f_e and f_h are the Fermi distributions of electrons and holes in the conduction and valence bands, and $f_i = [1 + \exp(\epsilon_i - \mu_i)/kT_i]^{-1}$ where $i = e, h$. The absorption constant α is linearly proportional to the optical density. In order to fit the experimental data in Fig. 1, 1.5 OD is subtracted from α_0 . We assume that the electrons and holes thermalized among themselves immediately after they were generated optically via carrier collisions and have a common temperature, $T_e = T_h$. This assumption is reasonable because electron-electron scattering can redistribute the momenta and the energies of free carriers in a very short time compared to the pulse duration so that the quasi-Fermi distributions can be reached by the free carriers.¹³ In the equation for f_i , ϵ_e and ϵ_h are the energies of electrons and holes, and μ_e and μ_h are the chemical potentials for electrons and holes, respectively. The carrier density for a degenerate distribution is

$$\eta = 2 \left(\frac{2\pi m_i k T_i}{h^2} \right)^{3/2} \mathcal{F}_{1/2} \left(\frac{\mu_i}{k T_i} \right), \quad i = e, h$$

where

$$\epsilon_e = \frac{(\hbar\omega - \bar{E}_g)m_h}{m_e + m_h}, \quad \epsilon_h = \frac{(\hbar\omega - \bar{E}_g)m_e}{m_e + m_h},$$

and $\mathcal{F}_{1/2}(\mu_i/kT_i)$ is the Fermi function. The effective masses¹⁴ of electrons and holes in the direct band of GaSe are $m_e (=0.2m_0)$, $m_h (=0.5m_0)$, where $m_i = (m_{i\perp}m_{i\parallel})^{1/3}$, and $m_{i\perp}$ and $m_{i\parallel}$ are the effective masses of carrier i ($i = e, h$) normal or parallel to the c axis of GaSe. The reduced band gap is \bar{E}_g , and $\hbar\omega$ is the probe pulse photon energy.

The theoretical fits to the data are described as follows: in Fig. 1(b), the best fit of the experimental data to Eq. (1), occurs when $T_e = T_h = 2000$ K, $\eta = 10^{19}$ cm⁻³, and $\bar{E}_g = 1.950 \pm 0.01$ eV for 0-ps delay; in Fig. 1(c), $T_e = T_h = 1700$ K, $\eta = 9 \times 10^{18}$ cm⁻³, and $\bar{E}_g = 1.950 \pm 0.01$ eV for 10-ps delay; in Fig. 1(d), $T_e = T_h = 1000$ K, $\eta = 8 \times 10^{18}$ cm⁻³, and $\bar{E}_g = 1.955 \pm 0.01$ eV for 30-ps delay; in Fig. 1(e), $T_e = T_h = 600$ K, with $\eta = 7 \times 10^{18}$ cm⁻³, and $\bar{E}_g = 1.955 \pm 0.01$ eV for 50-ps delay; in Fig. 1(f), $T_e = T_h = 320$ K, with $\eta = 6.5 \times 10^{18}$ cm⁻³, and $\bar{E}_g = 1.955 \pm 0.01$ eV for 100-ps delay; in Fig. 1(g), $T_e = T_h = 300$ K, with $\eta = 3 \times 10^{18}$ cm⁻³, and $\bar{E}_g = 1.960 \pm 0.01$ eV for 150-ps delay; in Fig. 1(h), $T_e = T_h = 300$ K, with $\eta = 7 \times 10^{17}$ cm⁻³, and $\bar{E}_g = 1.965 \pm 0.01$ eV for 250-ps delay. The change in the carrier density arises from the recombination of carriers due to stimulated emission occurring within 100 ps. The carrier density $\eta = 10^{19}$ cm⁻³ at $t = 0$ ps is close to the estimated value calculated earlier from measured values. The reduced band gap \bar{E}_g is obtained for carrier density below 10^{18} cm⁻³ from⁹ luminescence peak minus $\frac{1}{2}kT$. The carriers cooled down in less than 100 ps to 300 K, which is the lattice temperature. The theoretical fit to the experimental results shown in Fig. 1 by Eq. (1) is sensitive to changes of the carrier density η but not to the change of reduced band gap \bar{E}_g . The calculated curves are similar for changes in \bar{E}_g by as much as ± 10 meV. In Fig. 2, the carrier temperature T_e as a function of the time delay is drawn. The carrier temperature cools at a rate of 30 K/ps. The temperature decay time is 42 ps. If we assume that the carrier density remains 10^{19} cm⁻³ for the first 100 ps, then the carrier temperature will decay at a rate of 22 K/ps. In this case the temperature decay time would be 58 ps.

The hot-carrier relaxation mechanism occurs from the emissions of optical and acoustic phonons. The average rate of change of carrier energy due to nonpolar optical-phonon interactions is¹⁵

$$\left\langle \frac{d\epsilon}{dt} \right\rangle_{op} = - \left(\frac{2}{\pi} \right)^{1/2} \frac{D^2 m_{\perp} m_{\parallel}^{1/2}}{\pi \hbar^2 MN} (kT_e)^{1/2} \times \frac{e^{x_0 - x_e} - 1}{e^{x_0} - 1} \frac{x_e}{2} K_1 \left(\frac{x_e}{2} \right) e^{x_e/2}, \quad (2)$$

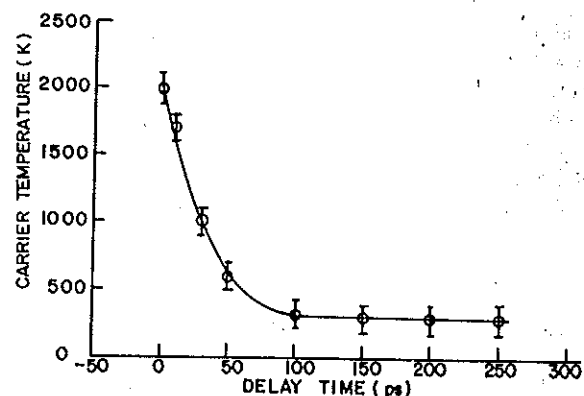


FIG. 2. Comparison of carrier temperature vs the delay time between the pump and probe pulses obtained from measurements (dots with error bars) of Fig. 1, and from theory (solid line) of Eq. (2).

where K_1 is a Bessel function of the second kind, $\chi_0 = \hbar\omega_0/kT$, $\chi_e = \hbar\omega_0/kT_e$, T and T_e are the temperatures of the lattice and the carriers, $\hbar\omega_0$ is the energy of the nonpolar optical phonon, D is the interaction constant or deformation potential having the dimensions of energy per length, M is the reduced ionic mass per unit cell, N is the number of cells per unit volume, and m_{\perp} and m_{\parallel} are the transverse and longitudinal masses of the carriers. In GaSe, $m_{\perp} = m_1$ and $m_{\parallel} = m_{\parallel}$. Following Schmid, we have replaced the crystal density (5 g/cm³) in Eq. (2) by MN (~ 2.2 g/cm³) (Ref. 4) because the interaction matrix of carrier-optical phonon is different for layer compound and each unit cell is treated as an independent oscillator with a reduced mass.^{2,4} Since the electrons and holes in the conduction and valence bands are Fermi gases, the average energy $\langle \epsilon \rangle$ for each pair of electron and hole¹⁶ is $\sim 3kT_e$. It is reasonable to substitute in Eq. (2) $\langle d\epsilon/dt \rangle$ by $3kdT_e/dt$ with $\chi_e/2 \ll 1$ and $K_1(\chi_e/2) \sim 2/\chi_e$. Equation (2) is used to fit the experimental data in Fig. 2 to obtain the relaxation of the carrier temperature. The dots with error bars represent the experimental results and the solid line represents the solution of Eq. (2). We found the coefficient

$$\frac{1}{3} \left(\frac{2}{\pi} \right)^{1/2} \frac{D^2 m_{\perp} m_{\parallel}^{1/2}}{\pi \hbar^2 MN} k^{-1/2} = 1.11 \times 10^{12}$$

and $\hbar\omega_0 = 16.7$ meV fits the experimental data very well. Therefore, the dominant relaxation mechanism of the photogenerated hot carriers is the emission of nonpolar optical phonons $A_1^{(1)}$ with an energy of 16.7 meV.

Using known parameters and the coefficient 1.11×10^{12} the interaction constant, D , between the holes and the nonpolar optical phonons is calculated to be about 1.3 eV/Å. The value of $D = 1.3$ eV/Å between the holes and the nonpolar optical phonons

is about five times smaller than the result measured by Schmid and Voitchovsky⁴ (~ 6.6 eV/Å). The value of D deduced by Schmid⁴ was from the Hall mobility of holes parallel to the layers in ϵ -GaSe when the impurity hole concentration is of the order of 3×10^{17} cm⁻³. A reasonable explanation for the difference between our value of D and Schmid's value is that the interaction strength between the holes and the nonpolar optical phonons is screened by the photogenerated carrier concentration which in our case is 30 times larger than Schmid's thermal hole density. We plan to perform measurements on time-resolved luminescence from GaSe at different excitation intensities to support our speculation. We should observe slower rise times of the luminescence under higher excitations if the dominant relaxation mechanism for the hot carriers is the emissions of

nonpolar optical phonons which are screened by photogenerated carriers.

In conclusion, we have observed that the dominant relaxation mechanism of photogenerated hot carriers is the emission of nonpolar optical phonons $A_1^{(1)}$ (~ 16.7 meV). The deformation potential interaction constant is less than that measured value at a lower concentration of carriers. Our lower value for D is attributed to the screening effect of phonons by the high density of photogenerated carriers.

ACKNOWLEDGMENTS

We thank the Air Force under Grant No. AFOSR 80-0079 for support of this research, and Dr. J. C. Irwin of Simon Fraser University and Dr. R. Seymour for samples.

¹J. L. Staehli and A. Frova, *Physica (Utrecht)* **99B**, 299 (1980).

²Ph. Schmid, *Nuovo Cimento B* **21**, 258 (1974).

³M. Schlueter, *Nuovo Cimento B* **13**, 313 (1973).

⁴Ph. Schmid and J. P. Voitchovsky, *Phys. Status Solidi. (b)* **65**, 249 (1974).

⁵V. Angelli, C. Manfredotti, R. Murri, and L. Vasanelli, *Phys. Rev. B* **17**, 3221 (1978).

⁶G. Antoninoli, D. Bianchi, U. Emiliani, P. Podini, and P. Franzoni, *Nuovo Cimento B* **54**, 211 (1979).

⁷J. Shah and R. F. Leheny, *Phys. Rev. B* **16**, 1577 (1977).

⁸A. G. Doukas, V. Stefancic, J. Buchert, R. R. Alfano, and B. A. Zilinskas, *Photochem. Photobiol.* **34**, 505 (1981).

⁹S. S. Yao and R. R. Alfano (unpublished).

¹⁰B. L. Evans, in *Optical and Electrical Properties* (D. Reidel Publishing, Boston, 1976), Vol. 4.

¹¹T. Ugumori, K. Masuda, and S. Namba, *J. Phys. Soc. Jpn.* **41**, 1991 (1976).

¹²K. Arya and W. Hanke, *Phys. Rev. B* **23**, 2988 (1981).

¹³R. Ulbrich, *Phys. Rev. B* **8**, 5719 (1973).

¹⁴G. Ottaviani, C. Canali, F. Nova, Ph. Schmid, E. Mooser, R. Minder, and I. Zschokke, *Solid State Commun.* **14**, 933 (1974).

¹⁵E. M. Conwell, in *Solid State Physics*, edited by F. Seitz, D.

Turnbull, and H. Ehrenreich (Academic, New York, 1967), Suppl 9, p. 155.

¹⁶For parabolic energy bands

$$\langle \epsilon \rangle = \frac{1}{\eta} \int \rho(\epsilon) f(\epsilon) \epsilon d\epsilon$$

$$= \frac{1}{\eta} 2 \left(\frac{2\pi mkT}{h^2} \right)^{3/2} \int_0^\infty \frac{\epsilon (\epsilon/kT)^{1/2} d(\epsilon/kT)}{1 + \exp[(\epsilon - \mu)/kT]}$$

$$\eta = 2 \left(\frac{2\pi mkT}{h^2} \right)^{3/2} \int_0^\infty \frac{(\epsilon/kT)^{1/2} d(\epsilon/kT)}{1 + \exp[(\epsilon - \mu)/kT]} \sim 10^{19} \text{ cm}^{-3}$$

when $\mu \leq 0$,

$$\eta \approx 2 \left(\frac{2\pi mkT}{h^2} \right)^{3/2} \frac{\sqrt{\pi}}{2} \exp\left(\frac{\mu}{kT}\right)$$

and

$$\langle \epsilon \rangle = \frac{1}{\eta} 2 \left(\frac{2\pi mkT}{h^2} \right)^{3/2} (kT) \exp\left(\frac{\mu}{kT}\right) \frac{3}{4} \sqrt{\pi} \approx \frac{3}{2} kT$$

for holes, $\mu_h \leq 0$ when $T_h \geq 370$ K; and for electrons, $\mu_e \leq 0$ when $T_e \geq 930$ K.